Fabrication and Interfacial Properties of Polymer Brush Gradients by Surface-Initiated Cu(0)-Mediated Controlled Radical Polymerization

Ella S. Dehghani,[†] Yunhao Du,[‡] Tao Zhang,[‡] Shivaprakash N. Ramakrishna,[†] Nicholas D. Spencer,[†] Rainer Jordan,*[‡] and Edmondo M. Benetti*[†]

[†]Laboratory for Surface Science and Technology, Department of Materials, Swiss Federal Institute of Technology (ETH) Zürich, Vladimir-Prelog-Weg 1-5/10, CH-8093 Zürich, Switzerland

[‡]Chair of Macromolecular Chemistry, School of Science, Technische Universität Dresden, Mommsenstrasse 4, 01069 Dresden, Germany

S *Supporting Information*

ABSTRACT: Surface-initiated Cu(0)-mediated controlled radical polymerization (Si-CuCRP) can be successfully applied to fabricate poly[(oligoethylene glycol)methyl ether methacrylate] (POEGMA) brushes in one pot, presenting a grafting-density gradient across the surface. This is achieved by continuously varying the distance (d) between a copper plate, used as a source of Cu species, and the initiator-functionalized substrate. X-ray photoelectron spectroscopy (XPS) analysis of monolayers of Cu^I-selective ligands demonstrates that a higher concentration of activator species diffuses to the initiating substrate in areas closer to the copper plate, a progressive decrease in activator concentration being observed upon increasing the distance between the two surfaces. As confirmed by the SI-CuCRP kinetics measured at different positions along the gradient, radical-termination reactions between propagating chains limit the grafting density of POEGMA grafts where the diffusion of activators is favored (i.e., at $d \rightarrow 0$). This effect decreases with increasing d, ultimately yielding a gradual variation of POEGMA grafting density across the substrate. We have investigated the influence of grafting-density variation across the gradient on the swelling of POEGMA brushes as well as on their nanomechanical and nanotribological properties, measured by a combination of variable angle spectroscopic ellipsometry (VASE), colloidal-probe atomic force microscopy (CP-AFM), and lateral force microscopy (LFM). The results of these tests highlight how loosely grafted POEGMA chains incorporating a substantial amount of water can be significantly deformed by a shearing AFM probe, exhibit relatively high friction, and generate friction-vs-load (F_f–L) profiles that follow a sublinear trend described by a Johnson–Kendall–Roberts (JKR) model—typical of deformable films of high surface energy. In contrast, more densely packed POEGMA brushes incorporate less solvent and display very low friction, with F_f–L data following a linear progression according to Amontons' law.
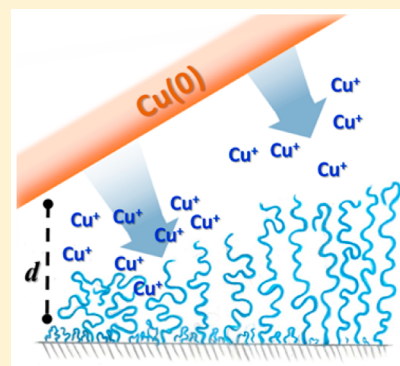
INTRODUCTION

Polymeric films presenting gradient characteristics have been largely applied for modulating the chemical, physical, and morphological properties of surfaces in a spatially defined fashion and within one single platform.[1−4] Especially surface gradients constituted by polymer brushes were employed to control the interaction with biological media, e.g., varying the adsorption of proteins and the adhesion of cells in a gradual way across a substrate.[5−8] In particular, polymer brush characteristics such as brush thickness (h) and grafting density (σ) determine the steric stabilization of the surface and thus regulate the interaction with biological entities. These parameters can be precisely modulated along a brush gradient by exploiting the intrinsic control granted by surface-initiated controlled radical polymerizations (SI-CRP) and/or by varying the initiator coverage on the underlying substrate.[9,10] Besides being applied for designing biointerfaces that stimulate a gradual variation of biological phenomena, polymer brush gradients are intrinsically interesting as fundamental study

platforms for dissecting the interfacial physicochemical properties of grafted polymers presenting variable characteristics.

In this study, we applied Cu(0)-mediated controlled radical polymerization (CuCRP) to generate structural gradients of poly[(oligoethylene glycol)methyl ether methacrylate] (PO-EGMA) brushes on silicon oxide surfaces and subsequently investigate their interfacial physicochemical properties by a combination of surface sensitive techniques and atomic force microscopy (AFM)-based methods. Noteworthy, POEGMA is a technologically relevant polymer which combines the attractive characteristics of poly(ethylene glycol)s (PEGs) with the versatility of radically polymerizable monomers, and it was previously applied to fabricate biopassive surfaces and cell responsive coatings.[11−13]

Scheme 1. (a) SI-CuCRP of OEGMA Using a Tilted Cu Plate Generates a POEGMA Brush Grafting Density Gradient along the Substrate; (b) Mechanism of SI-CuCRP Follows the SARA-ATRP Process;[34] Cu(I)X/L Represents All The Cu(I)-Based Species Irrespective of Their Speciation, Cu(II)X2/L Represents All The Cu(II)-Based Species Irrespective of Their Speciation. (c) Chemical Compositions of the Initiator Monolayer and the Subsequently Grafted POEGMA Brush; (d) CSL Monolayers on Silicon Oxide Substrates are Applied in a Setup Similar to the One Used for SI-CuCRP for Immobilizing CuI Species Diffusing at the Surface from the Cu Plate[a]
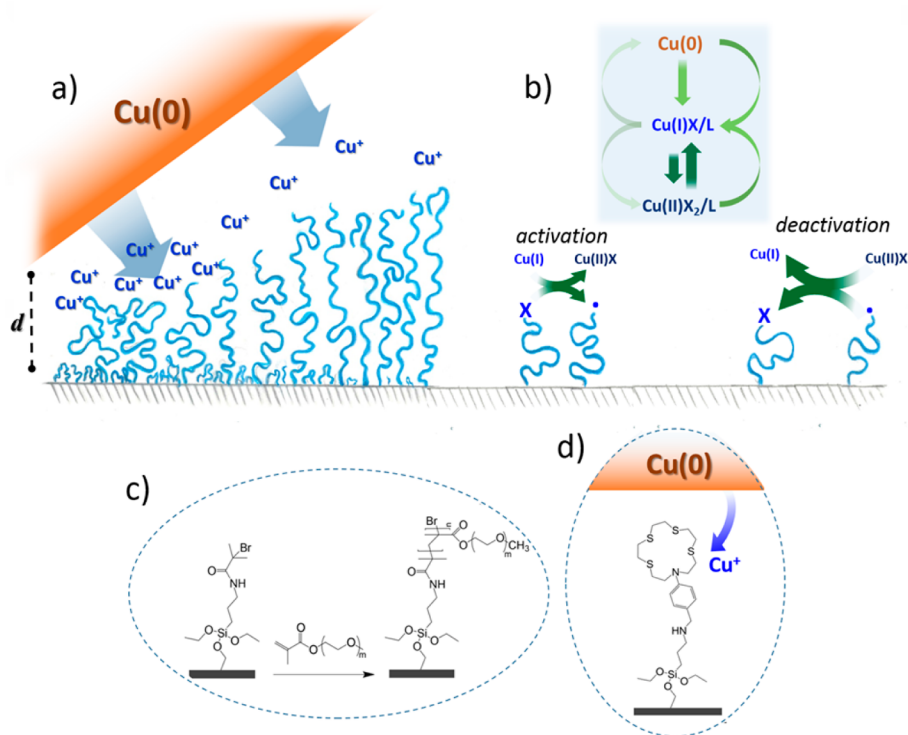
[a]XPS is subsequently applied to estimate the surface concentration of Cu[I] species.

In the first part of the paper, the one-pot fabrication of grafting-density gradients of POEGMA brushes by SI-CuCRP is presented. This process exploits very low concentrations of Cu species generated from a copper plate positioned above an initiator-functionalized surface to trigger the atom transfer radical polymerization (ATRP) equilibrium and the consequent growth of brushes.[14] Here we demonstrate that a variation of the vertical distance between the metallic plate and the initiating surface (plate tilting) stimulates a corresponding, gradual variation in brush grafting density due to differences in the local concentration of activator and deactivator Cu species.

In the second part of the paper, we focus on the comprehensive characterization of the interfacial physicochemical properties of the generated brush gradients. A thorough understanding of how nanoscale swelling as well as mechanical and tribological properties are determined by the surface density of a polymer brush has not been fully achieved to date. Several reports have highlighted that the steric stabilization provided by hydrophilic brushes is increased by incrementing grafting density,[15,16] while friction decreases when the packing of chains is maximized.[7] Although these initial studies suggested that the osmotic barrier generated by a densely grafted brush is responsible for its lubricious properties, an unambiguous understanding of how a precise tuning of brush structural parameters translates into variations in the adhesive, mechanical, and frictional properties of the functionalized surfaces is currently missing. In order to comprehensively investigate the effects of brush structural variation on interfacial properties, we

have applied SI-CuCRP to the fabrication of POEGMA brush-density gradients and provided a full characterization of their interfacial properties by a combination of variable angle spectroscopic ellipsometry (VASE), AFM nanoindentation, and lateral force microscopy (LFM). In particular, the nanotribological properties of POEGMA brushes, studied by LFM, were found to correlate with brush swelling, the lateral deformability of the grafts, and their nanomechanical characteristics across the gradient surface. Continuum contact-mechanics models are applied to describe friction-vs-load (F_f−L) profiles and how friction varies in response to a modulation of brush grafting density. Loosely grafted POEGMA brushes swell profusely in water and do not efficiently passivate the underlying substrate. In this regime, friction is high because of the low osmotic pressure within the assembly, while it increases sublinearly with the applied load, following Johnson−Kendall−Roberts (JKR) contact-mechanics behavior. An increase in grafting density along the gradient translates into a decrease in brush swelling (i.e., more highly stretched and packed chains) and a concomitant reduction of friction, with dense brushes showing highly lubricious behavior and generating linear F_f−L profiles, in accordance with Amontons' law.

SI-CuCRP is a powerful and easily accessible synthetic tool for the fabrication, in one pot, of brush grafting-density gradients with great precision and high reproducibility. Exploiting the diffusion of Cu species from a metallic plate placed at determined distances from the initiating substrate, this

process features several advantages over the commonly applied SI-ATRP process: (i) it can be scaled up to large surfaces, (ii) it can be applied multiple times to produce a large number of identical gradients, and (iii) it does not require the use of soluble Cu-based catalysts or other potentially toxic compounds. By employing the most advanced AFM-based methods, we demonstrate that all these attractive characteristics make SI-CuCRP an ideal fabrication approach for the investigation of the influence of brush parameters on the nanomechanical and nanotribological properties of the generated polymer surface.

■ EXPERIMENTAL SECTION

Materials. Oligo(ethylene glycol) methyl ether methacrylate (OEGMA, Sigma-Aldrich, $M_n \sim 475$ g mol^{-1}) was purified from inhibitors by passing it through a basic alumina column ($\phi = 0.22$ μm). Methanol (Sigma-Aldrich, ≥99.8%), ethanol (VWR Chemicals, absolute), dichloromethane (DCM, dry, Acros, ≥99.8%), acetone (dry, Merck KGaA, ≥99.8), triethylamine (TEA, Sigma-Aldrich, ≥99.5%), 2-bromoisobutryl bromide (BiBB, Sigma-Aldrich, 98%), 3-(aminopropyl)triethoxysilane (APTES, Sigma-Aldrich, 99%), dimethyl sulfoxide (DMSO, VWR Chemicals, 99.6%), 1,1,4,7,7-pentamethyldiethylenetriamine (PMDETA, Acros, ≥98%), 3,7-dithia-1,9-nonanedithiol (Tokyo Chemical Industry, Japan), N,N-dimethylformamide (Aldrich, Germany), sodium borohydride (98+%, Acros, Germany), lithium hydroxide hydrate (Sigma-Aldrich, Germany), and 4-(bis(2-chloroethyl)amino)benzaldehyde (Sigma-Aldrich, Germany) were used as received. Cu plates (Micro Chemicals GmbH, Germany) with a thickness of 200 nm (purity >99.9%, RMS < 10 nm) were washed with ultrapure water, ethanol, and DMSO under ultrasonication (5 min) prior to use. After cleaning, Cu plates were immediately used for SI-CuCRP. Silicon wafers with an ∼300 nm oxide layer were purchased from Wacker AG (Burghausen, Germany). Alexa Fluor 546-labeled fibrinogen from human plasma (Thermo Fischer Scientific, Germany) was mixed with HEPES-2 buffer to yield 150 μg/mL concentration. Water used in all the experiments was Millipore Milli-Q grade.

Functionalization of SiO$_2$ Surfaces with ATRP Initiator. Silicon substrates were cleaned with piranha solution (H$_2$O$_2$:H$_2$SO$_4$ = 1:3 v/v, room temperature, 20 min; *Caution: piranha solution reacts violently with organic matter! Please use carefully!*), then washed extensively with Milli-Q water, and dried under a stream of dry nitrogen. The freshly cleaned substrates were immersed into a 5% (v/v) aminopropyltrimethoxysilane (APTES) solution in dry acetone and ultrasonicated under nitrogen for 45 min. After the formation of an APTES layer, the substrates were rinsed with dry acetone and dried under nitrogen. The substrates were subsequently immersed in 20 mL of dry DCM under nitrogen. 0.4 mL of TEA was added to the solution, followed by dropwise addition of BiBB (2% in DCM) at 0 °C under nitrogen. The mixture was then stirred at room temperature overnight. Subsequently, the substrates were rinsed with DCM, water, ethanol, and acetone and then dried under a stream of nitrogen. The functionalized silicon oxide substrates were subsequently used for SI-CuCRP.

Surface-Initiated Cu(0)-Mediated Controlled Radical Polymerization (SI-CuCRP). A Cu plate and an initiator-functionalized substrate were clamped together, maintaining a plastic spacer with a thickness of 1 mm at one end of the two facing surfaces. A gradual variation of distance between the two surfaces, i.e., from contact to 1 mm distance, was thus obtained (the setup is depicted in Scheme 1). The substrate was subsequently immersed in a solution of OEGMA (2 g, 0.1 mmol), solvent (2 mL of Milli-Q water and 1 mL of methanol), and ligand PMDETA (16.5 μL, 0.08 mmol), which had been previously deoxygenated by nitrogen bubbling for 30 min. After 1 h of polymerization at room temperature, the reaction was terminated by rinsing the silicon substrate with water and ethanol. The substrate was finally dried in a stream of nitrogen and further analyzed.

Synthesis of 13-(4-Formylphenyl)-1,4,7,10-tetrathia-13-aza-cyclopentadecane. The Cu(I)-complexing adsorbate 13-(4-formyl-phenyl)-1,4,7,10-tetrathia-13-azacyclopentadecane (copper selective ligand, CSL) was synthesized according to Fahrni et al.[17] Namely, 642 mg of 4-(bis(2-chloroethyl)amino)benzaldehyde, 735 mg of 3,7-dithia-1,9-nonanedithiol, and 360 mg of LiOH were mixed in 100 mL of DMF and were refluxed for 10 h. The solvent was then removed on a rotary evaporator, and the residue purified by column chromatography using silica gel with DCM and MeOH (v:v = 10:1) as eluent (H NMR spectrum of the CSL is provided in the Supporting Information).[18] APTES-functionalized silicon oxide substrates wafers were incubated in 10 mg/mL dichloromethane/methane (v:v = 3:1) solution of CSL containing 5 mM NaBH$_4$ overnight. Cu plates were subsequently clamped with the CSL-modified surfaces in a similar way to the substrates used for SI-CuCRP and later on incubated in a methanol:water (v:v = 2:1) mixture for an hour. Finally, the samples were washed with methanol and dried under a stream of nitrogen.

Characterization. The dry and swollen thickness of POEGMA brushes was measured with a variable-angle spectroscopic ellipsometer (VASE) from SENTECH Instruments GmbH, equipped with a He–Ne laser source ($\lambda = 633$ nm, J.A. Woollam Co., Lincoln, NE). The recorded spectra were modeled using SpectraRay 3 software. The film thickness was measured by recording amplitude (Ψ) and phase (Δ) components as a function of wavelength (275−827 nm) and applying a three-layer model featuring Si, SiO$_2$, and a Cauchy layer, using the known refractive indices of Si and SiO$_2$ (software WVASE32, LOT Oriel GmbH, Darmstadt, Germany).[19] A Cauchy model, $n = A + B/\lambda^2$, was used to describe the refractive index of the POEGMA films by means of two fitting parameters: offset ($A = 1.45$) and wavelength dispersion ($B = 0.01$). Measurements in water were carried out using a liquid cell containing two windows at a fixed angle of $\theta = 70°$. The swollen POEGMA thickness was measured using a graded effective medium approximation (EMA) model, which was based on a linear combination of the optical constants of Milli-Q water and the polymer film.

Colloidal-probe atomic force microscopy (CP-AFM) was employed to measure pull-off (adhesive) forces and the apparent Young's modulus (E) of the films, while lateral force microscopy (LFM) was applied to measure their nanotribological properties. In both cases an AFM Asylum Research was used (MFP-3D, Santa Barbara, CA). Colloidal probes were prepared by mounting silica spheres (Kromasil, Brewster, NY, diameter = 20 μm) onto tipless, Au-coated silicon cantilevers (Micromash, San Jose, CA) with a homemade micromanipulator and a UV-curable adhesive (Norland optical adhesive 61). The normal spring constant of Au-coated tipless cantilevers (NSC-36, Micromasch, Estonia) was measured by the thermal-noise method,[20] and the torsional spring constant was measured according to Sader's method.[21] Both normal and torsional spring constants of the cantilevers were measured before attaching the silica microspheres. The elastic and adhesive properties of brush films were measured from the approaching and retracting profiles of the recorded force-vs-distance (F–D) curves (30 force curves over 20 μm × 20 μm area, in a minimum of three spots). The apparent Young's modulus (E) of the POEGMA brush gradient films was estimated by using the Hertz model,[22] provided in the instrument software (Asylum Research, AR12), fitting the approaching profiles of the F–D curves between the contact point and an indentation depth corresponding to less than 10% of the film swollen thickness, by applying the following equation:

$$F = \frac{4ER^{0.5}\delta^{1.5}}{3 - 3\nu^2} \tag{1}$$

where F is the applied force, R is the radius of the colloid used as a probe, and ν is Poisson's ratio of the polymer (considered as 0.5).

The lateral force calibration was performed according to the method described by Cannara et al.[23] To determine the lateral sensitivity of the photodetector, a freshly cleaned silicon wafer (1 cm × 1 cm) was glued "edge-on" to a glass slide. The smooth silicon plane was used as a "wall" for measuring the lateral sensitivity. A test probe (cantilever glued with a silica sphere of diameter around 40 μm) was moved
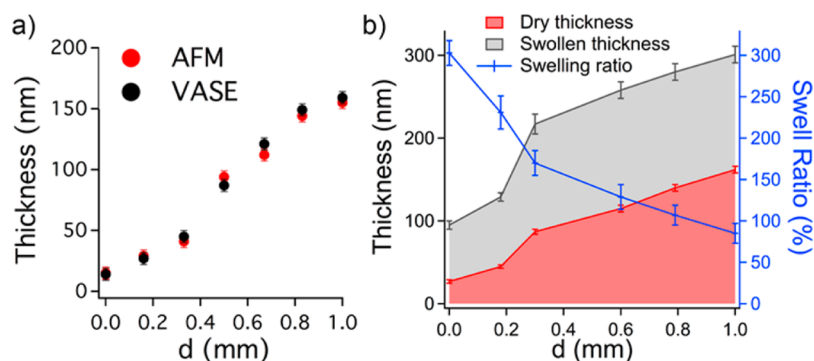
Figure 1. (a) Dry thickness of POEGMA made by SI-CuCRP, measured by VASE and AFM along the gradient substrate at different separations between substrate and copper plate, from $d \sim 0$ to $d \sim 1$ mm. (b) Comparison of dry thickness, wet thickness, and the swelling ratio measured by VASE.

laterally into contact with the silicon wall without interacting with the glass surface below. The slope of the obtained lateral-deflection versus piezo-displacement curve yielded the lateral sensitivity used for lateral-force calibration. The friction-force measurements were performed by scanning the probe laterally and applying different loads at a constant speed 3 μm s^{-1}, in at least four different spots on each substrate, recording 10 friction force "loops" on each spot. The measurements of brush lateral deformation were conducted by applying a similar setup with the exception of the scanning rate, which was set at 0.5 μm s^{-1}.

For the AFM step-height measurements, plastic tweezers were used to mechanically remove the polymer films, exposing the underlying silicon oxide surface below. Following the film's removal, tapping-mode AFM (Bruker Dimension Icon, cantilever used BL-AC40TS-C2, Olympus, Japan, $k = 0.09$ N m^{-1}, $f = 110$ kHz in air, tip radius <10 nm) was used to scan areas on the samples where both the scratched region and intact polymer film were present.

The swelling properties of POEGMA brushes were confirmed by step-height AFM measurements, performed in dry state and in Milli-Q water. The swelling ratio of POEGMA brushes was thus calculated as the difference between dry and swollen thickness, divided by the dry thickness.

The POEGMA brush grafting density (σ) was estimated according to eq 2:[24]

$$\sigma = \rho_0 h_{dry} N_A ((0.227(T_{wet})^{1.5}(T_{dry} \ (Å^2))^{-0.5})M_0)^{-1} \quad (2)$$

where ρ_0 is the dry density of POEGMA (1.40 g cm^{-3}), N_A is Avogadro's number, M_0 is the monomer molecular weight (475 g mol^{-1}), and 0.227 is a constant related to the excluded volume parameter ($\omega = 7$ Å^3), a constant $\nu = (a^2/3)^{-1}$, where a represents the Kuhn length of the monomer unit (10.5 Å for POEGMA).[25] The dry and swollen thicknesses were measured by VASE under dry conditions or in Milli-Q water, respectively.

Static water-contact-angle (WCA) measurements were performed with a drop-shape analysis system (DSA 10, Krüss). For each sample, individual measurements at three different areas were performed and averaged. Contact-angle measurements were performed at room temperature with Milli-Q water, and the contact angles were obtained using the tangent method fitting.

X-ray photoelectron spectroscopy (XPS) measurements were performed with a Theta-Probe X-ray photoelectron spectrometer (ARXPS, Thermo Fisher Scientific, Waltham MA), equipped with a monochromatic Al Kα source and a beam diameter of 300 μm. The pass energy was 100 eV for the high-resolution spectra of sulfur, copper, nitrogen, carbon, and oxygen elemental analysis, while the pass energy of the survey spectrum was 200 eV. An electron-argon-ion flood gun was used to compensate for the charging occurring at the surface. Eight spots along the wafer, with an average distance of 1 mm from each other, were measured, in the standard lens mode with an emission angle of 53° to the surface and an acceptance angle of ±30°.

Protein Adsorption on POEGMA Brush Gradients. The antifouling properties of POEGMA films were studied by fluorescence

microscopy (using Axio IMAGER M1m, Zeiss, Oberkochen, Germany), monitoring the adsorption of fluorescently labeled fibrinogen (Fgn). ImageJ software (open source from www.imagej.net) was used to measure the relative intensity of the fluorescence micrographs. The amount of protein adsorbed was evaluated by subtracting the fluorescence intensity recorded on each film before incubation in the protein solution from that recorded following protein adsorption.

■ RESULTS AND DISCUSSION

POEGMA Brush-Gradient Synthesis and Characterization. POEGMA brush gradients were fabricated by SI-CuCRP, following the experimental procedure that was already described by Jordan and co-workers.[14] Namely, a Cu plate was placed in proximity of the initiator-functionalized substrate by clamping the two surfaces together. The introduction of a glass spacer (1 mm in height) at one side of the clamped substrates allowed a gradual variation of distance (d) between the Cu source and the initiating surface. The diffusion of Cu species in the solution containing OEGMA and PMDETA enables the ATRP equilibrium and the subsequent polymerization from the initiator-functionalized substrates.[14,26] The mechanism of CuCRP proceeds according to the supplemental activator and reducing agent ATRP (SARA ATRP). This process involves mainly the activation/deactivation equilibria of Cu^I/Cu^{II} species, determining the formation of active radicals and their concentration, with a contribution of Cu^0 both as reducing agent for Cu^{II} (comproportionation to regenerate Cu^I, as depicted in Scheme 1) and as supplementary radical activator.[27−29] The versatility of SI-CuCRP allows the preparation of brushes from a broad variety of monomers such as acrylates, methacrylates, and acrylamides (Scheme 1).[11,35] When this process was carried out from initiators immobilized on a flat surface, the distance between the Cu source and the grafting substrate determines the polymer film thickness.[26] This could be gradually varied across a single substrate to yield a brush gradient by simply positioning a Cu plate antiparallel with respect to the initiating surface.[26]

Incubation of the Cu plate coupled to the initiating substrate for 60 min in a water/methanol solution of OEGMA and PMDETA resulted in a POEGMA brush film presenting a gradient of dry thickness ranging from 11 ± 1 nm (at $d \sim 0$) to 162 ± 3 nm (at $d \sim 1$ mm), as reported in Figure 1a. The variation of the brush swollen thickness along the gradient was proportionally less marked, T_{wet} varying from 84 ± 2 at $d \sim 0$ to 301 ± 4 nm at $d \sim 1$ mm, as measured by VASE and confirmed by AFM step height in Milli-Q water (Figure 1a,b). By

comparing the values of T_{dry} and T_{wet} at each measured position across the gradient, we could derive the variation in swelling ratio (S_r) (Figure 1b). The values of S_r progressively increased with decreasing the distance d between the Cu plate and the grafting surface. This result suggested that the POEGMA grafting density was not constant across the gradient substrate.[32]

To further investigate the effect of the distance between the Cu plate and the initiator-modified wafers (d), four polymerization sets were designed, in which SI-CuCRP was carried out keeping constant d at four different values (Table 1). After 1 h

Table 1. Dry (T_{dry}) and Swollen Thickness (T_{wet}), Swelling Ratio (S_r (%) = $100(S_t - D_t)D_t^{-1}$), and Estimated σ of POEGMA Brushes Synthesized by SI-CuCRP Keeping d Constant

d (mm)	T_{dry} (nm)	T_{wet} (nm)	S_r (%)	σ (chains nm^{-2})
contact point	30 ± 2	100 ± 5	233 ± 25	0.12
0.2	60 ± 4	149 ± 5	148 ± 20	0.19
0.5	166 ± 10	303 ± 12	84 ± 15	0.31
1	279 ± 5	420 ± 7	49 ± 5	0.42

of immersion in a polymerization medium similar to that applied for gradient fabrication, POEGMA brushes characterized by large deviations of thickness and S_r were obtained. Generally, the results of the control experiments confirmed the swelling behavior of POEGMA brushes recorded across the gradient samples, where small values of d led to thinner films that presented higher values of S_r. In particular, decreasing d from 1 mm to quasi-contact between the two surfaces ($d \sim 0$) translated into a more than 3-fold increment in S_r (Table 1). The estimate of σ according to eq 2 (see Experimental Section for details) resulted in values ranging from 0.12 to 0.42 chains nm^{-2} (Table 1) and thus confirmed how a decrease of d was accompanied by a substantial reduction of tethered-chain density, as also indicated from the values of σ calculated along the POEGMA brush gradient (Table 2).

Table 2. Dry (T_{dry}) and Swollen Thickness (T_{wet}), Swelling Ratio (S_r (%) = $100(S_t - D_t)D_t^{-1}$), and Estimated σ Measured at Different Points along a POEGMA Brush Gradient Synthesized by SI-CuCRP

d (mm)	T_{dry} (nm)	T_{wet} (nm)	S_r (%)	grafting density (chains nm^{-2})
contact point	30 ± 2	120 ± 5	300 ± 25	0.09
0.1	45 ± 2	151 ± 5	231 ± 20	0.12
0.4	96 ± 3	248 ± 12	158 ± 15	0.19
0.6	120 ± 4	278 ± 10	129 ± 15	0.22
1	162 ± 3	301 ± 10	85 ± 12	0.31

A change in σ was necessarily correlated with a different diffusion of Cu species to the surface-immobilized initiators as a function of d and consequently with the influence of their local concentration on the grafting process. Keeping in mind that no Cu salts were added to the polymerization mixture and that the major source of activation was derived from Cu^I/PMDETA complexes originated from the Cu plate, the accumulation of activators in the vicinity of the alkyl-halide-bearing monolayer and its dependency on d regulated the surface concentration of propagating chains. This is especially valid in aqueous media, where low control over the ATRP process is achieved. Under

these conditions, the large value of the ATRP equilibrium constant caused a high concentration of radicals and a relatively low "effective" concentration of Cu^{II}-based deactivating complexes.[33] Thus, a higher local concentration of Cu^I activators in areas of the initiating surface closer to the Cu plate (i.e., at smaller d values) would lead to a relatively high concentration of radicals.[33] Because of the confinement of the propagating radicals on a bidimensional surface, the occurrence of radical termination between neighboring chains is expected to become dominant, ultimately affecting σ. In particular, we believe that the occurrence of radical termination reactions is especially relevant during the first stages of the SI-CuCRP process, when the active chain ends of relatively low-molar-mass grafts are close enough to react between each other. As a general consequence, a gradual variation in the local concentration of Cu^I species along the initiating substrate (which was enabled by a progressive change of d) led to the formation of a gradient of σ (as estimated in Table 2).

To demonstrate this hypothesis, a silicon oxide substrate functionalized with a monolayer of silane-based copper-selective ligand (CSL)[17] was clamped with a tilted Cu plate (Scheme 1), in a similar setup as the one applied for CuCRP, and subsequently incubated for 1 h in the same polymerization mixture used for the gradient fabrication (without OEGMA). The surface concentration of Cu^I species immobilized at the monolayer was later on evaluated at different positions across the substrate (at different d) by X-ray photoelectron spectroscopy (XPS) (Figure 2 and Supporting Information).

As shown in Figure 2, the XPS elemental analysis indicated that the highest surface concentration of Cu^I (I_{Cu}) was recorded at $d \sim 0$, i.e., in areas of quasi-contact between the Cu plate and the substrate. In addition, an increase of d was accompanied by a progressive decrease of I_{Cu}. It is noteworthy that the recorded surface concentration profile of Cu^I species along the substrate followed closely the variation of S_r measured across a POEGMA brush gradient fabricated by SI-CuCRP using a similar setup (and thus the variation of σ) (Figure 1b).

Hence, we could conclude that a variation of d affected the local concentration of Cu^I species at the initiating substrate, to an extent such that the contribution of radical termination reactions to σ progressively varied along the surface. This was also proved by monitoring the thickening rates of POEGMA brushes measured at different positions across the brush gradient substrates. As reported in Figure 3, the rate of SI-CuCRP (indicated by the slope of the T_{dry}-vs-time profiles) steadily decreased by decreasing d, suggesting that radical termination reactions influenced the grafting process to a larger extent when the Cu plate approximated the initiating surface.[35,36]

Interfacial Properties of POEGMA Brush Gradients. Having established how CuCRP could be conveniently applied to fabricate grafting density gradients of POEGMA brushes, we subsequently investigated their interfacial physicochemical properties along the gradient direction. First, we confirmed the formation of gradients of POEGMA grafts by testing the adsorption of proteins across the substrates. POEGMA brushes have been largely applied to synthesize biopassive coatings that efficiently hinder the adsorption of proteins on the functionalized surfaces.[37−39] As a prerequisite for reaching sufficient biopassivity, the grafting density of POEGMA brushes must be high enough to guarantee efficient screening from the adsorbing proteins, a reduction of POEGMA grafting density
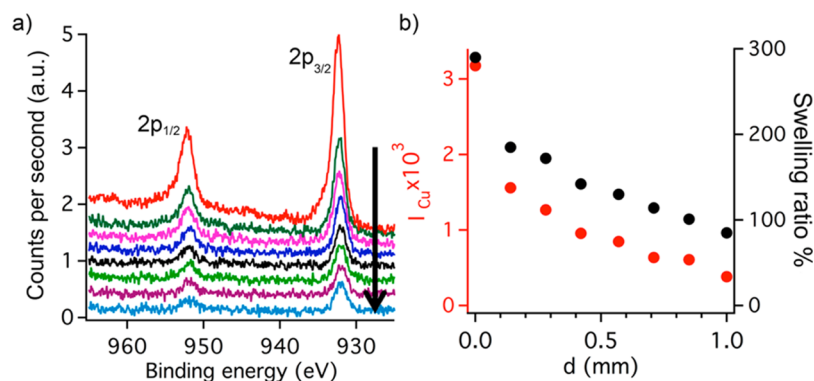
Figure 2. (a) Cu 2p peak signals measured with XPS along a CSL monolayer on silicon oxide; the arrow indicates the increase distance (d) from the Cu plate. (b) Area of Cu^I-related peaks (I_{Cu}) measured by XPS at positions presenting different d values. I_{Cu} at each point was normalized by the atomic sensitivity factor of Cu 2p for a X-ray source at 54.7°. The corresponding values of S_r for POEGMA brushes are also provided.
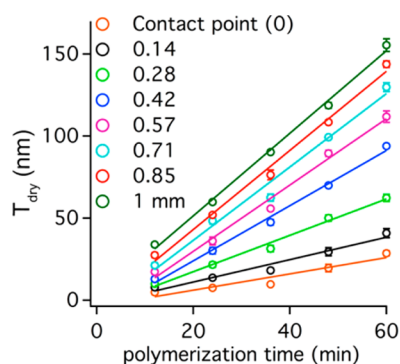
Figure 3. POEGMA brush thickening rates along the gradient as measured by VASE.

enabling the interaction of biomolecules with the underlying substrate and their subsequent "primary" adsorption.[40]

In order to test protein adsorption on POEGMA gradients, we used fluorescently labeled fibrinogen (Fgn) as a protein source and monitored its adsorption along the gradient by fluorescence microscopy (see Experimental Section for details). Specifically, POEGMA brushes were incubated in a 150 μg mL^{-1} solution of Fgn for 2 h, with the fluorescence intensity subsequently being measured at several positions along the gradients. As reported in Figure 4, the highest fluorescence intensity of adsorbed proteins was measured on POEGMA brushes corresponding to small values of d (i.e., where the estimated σ was low). In contrast, the intensity of the adsorbed proteins progressively decreased along the POEGMA gradient, following the increment of d applied during the SI-CuCRP
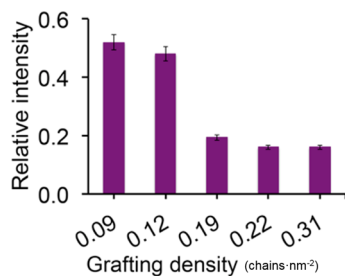
Figure 4. Relative fluorescence intensity of Fgn adsorbed along the POEGMA brush gradient. The corresponding estimated values of σ are indicated in the x-axis.

synthesis. This result confirmed how the increase of σ across the POEGMA brush substrate translated into a concomitant decrease in protein adsorption due to the increasingly efficient shielding of the underlying substrate by denser POEGMA brushes.

The nanomechanical and nanotribological properties of POEGMA brush gradients were subsequently investigated by a combination of colloidal-probe atomic force microscopy (CP-AFM) and lateral force microscopy (LFM). We especially focused on how the progressive variation of brush grafting density determined adhesion, brush stiffness, and friction.

From the retraction profiles of the recorded force-vs-distance (F−D) curves, the adhesion force between the colloidal probe and the POEGMA brushes could be measured. Moving across the POEGMA brush gradient from areas characterized by low σ toward regions with higher σ, a gradual decay in adhesion from 12 ± 2 to 1 ± 0.5 nN was measured (Figure 5). The relatively high adhesion measured for low-grafting-density POEGMA brushes was likely due to two contributions. On the one hand, loosely grafted chains did not efficiently passivate the underlying substrate, and thus the presence of surface defects on the brush assembly could be sensed by the retracting probe as an increase of adhesion. On the other hand, diluted grafts interacting with the silica probe via hydrogen bonding and van der Waals forces could be stretched out by the retracting probe from their equilibrium, coiled conformation to a larger extent if compared to more densely packed brushes.[41,42] Remarkably, the normal stretching of loosely grafted POEGMA chains by the retracting probe was recorded across several hundred nanometers. We believe that these long-range, adhesive interactions were mainly caused by polymer bridging between longer grafts within an intrinsically polydisperse assembly and the AFM probe.

It is important to emphasize that the grafted-chain length (degree of polymerization, DP) of POEGMA brushes is also expected to vary across the gradient surfaces due to the different kinetics of the CuCRP process. However, the contribution of a variation of DP is presumably much less relevant compared to the much steeper deviation of σ, which affects to a large extent the resistance toward protein adsorption, the underlying substrate screening, and the osmotic pressure within the brush.

The approaching profiles of the F−D curves were subsequently analyzed to estimate the stiffness of POEGMA brushes across the σ gradient (see Experimental Section for details). As shown in Figure 6, the approaching curves showed
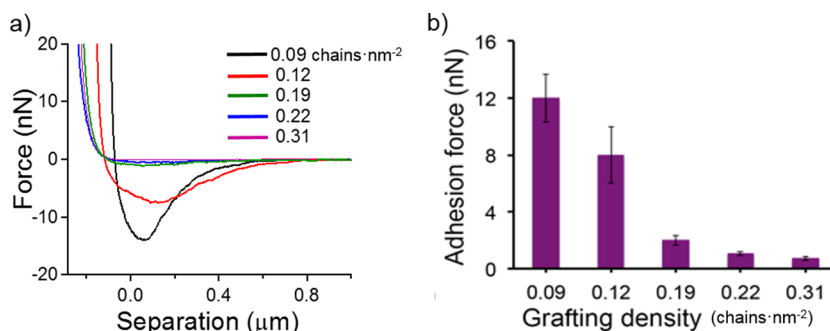
Figure 5. (a) Retraction profiles from $F–D$ curves recorded by CP-AFM on POEGMA brush gradient. (b) Average adhesion force measured along the POEGMA brush gradient (spring constant of the cantilever used 1 N m^{-1}, radius of the silica colloidal probe 8 μm, measured in Milli-Q water).
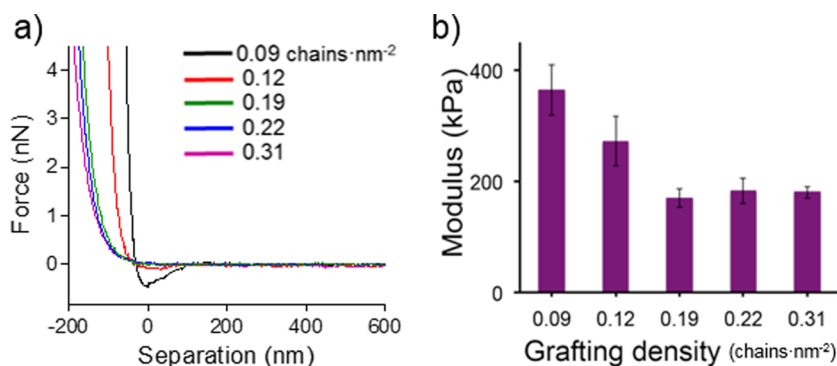
Figure 6. (a) Approaching profiles from $F–D$ curves (expressed as force-vs-penetration curves) recorded at different positions along the POEGMA brush gradient surface. (b) Estimated apparent Young's modulus (E) values for POEGMA brushes along the gradient surfaces.
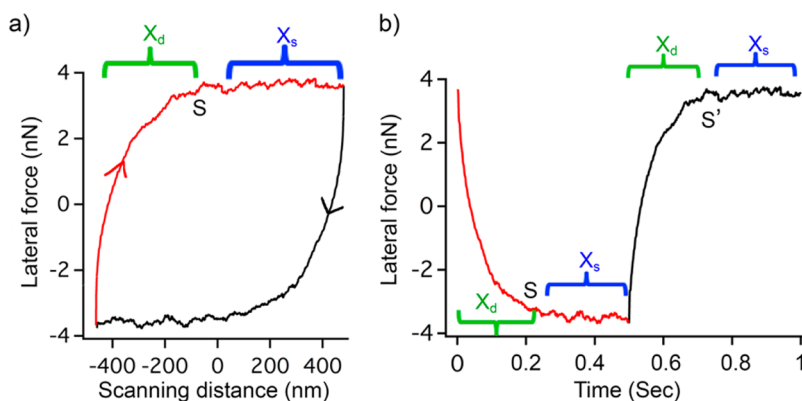
Figure 7. (a) A representative friction loop recorded by LFM on a swollen POEGMA brush applying a scanning rate of 1 μm s^{-1}. X_d and X_s indicate the scanning distances corresponding to the brush lateral deformation (tilting and stretching) and steady sliding, respectively. Point S indicates the transitions between these two regimes, and the scanning direction is shown by the arrows on both trace and retrace profiles. (b) Lateral force-vs-time during the recording of the same friction loop shown in (a).[44]

an increasing steepness after contact, upon decreasing the brush density. As previously observed by Sui et al.,[43] this was presumably due to the underlying substrate effect, the heterogeneous polymer coverage not efficiently screening the grafting surface in the case of low σ. As a consequence, the estimated, apparent Young's modulus (E) progressively increased with the decrease of grafting density, ranging from 364 ± 45 kPa at σ = 0.09 to 182 ± 23 kPa for σ = 0.31 (see Experimental Section for details).

Later on, we applied LFM to scrutinize the nanotribological properties of POEGMA brushes and the way in which these would be influenced by variation in the value of σ along the gradient substrates. We first evaluated the lateral deformability of POEGMA grafts, this quantity being measurable through the

analysis of the friction force loops recorded by LFM.[44,45] When swollen polymer brushes are subjected to a shearing AFM probe during LFM, the subsequently recorded friction force loops showed a tilted profile upon scanning-direction reversal (Figure 7).[46] This tilt originates from brush bending and stretching along the scanning direction and is correlated to the tethered chain length and brush swelling.[44] Following the friction force trace recorded during a loop, the swollen brush is initially deformed until the spring force of the bent brush reaches a maximum and overcomes the static friction, after which steady sliding is finally attained (point S in Figure 7). When the maximum lateral deformation of the brush (X_d in Figure 7) is normalized by its equilibrium swollen thickness

(T_{wet}), the brush lateral strain or the lateral deformability can be calculated.

The lateral strains of POEGMA brushes plotted as a function of the recorded lateral force, and measured at different positions along the grafting density gradient, are reported in Figure 8. It is worthy of note that values of lateral strain >1
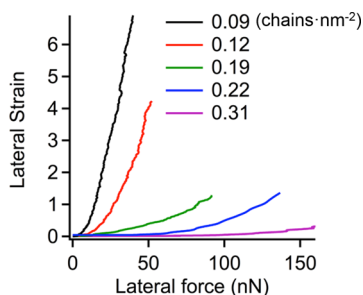
Figure 8. Brush lateral strain-vs-lateral force measured along the POEGMA brush gradient by LFM. The lateral strain is measured by normalizing the tilted section of the corresponding friction loop (X_d) by the equilibrium swollen thickness of the same brush (T_{wet}).

indicated that POEGMA brushes under shear could be laterally deformed well beyond their unperturbed, equilibrium extension, which was in accordance with previous experimental and simulation studies.[47,48]

As reported in Figure 8, the lateral deformability of POEGMA brushes substantially increased with decreasing brush grafting density, implying that loosely grafted chains can be laterally deformed to a larger extent compared to more densely packed brushes. At low values of σ, the grafts are not stretched from the grafting surface and rather resemble polymer coils attached to the surface. In this configuration, the shearing AFM probe was capable of laterally bending and stretching them to more than 6 times their equilibrium swollen thickness before sliding occurred. In contrast, the maximum lateral deformability of dense brushes ($\sigma = 0.31$ in Figure 8) was no more than ~10% of their fully stretched length, suggesting that densely packed grafts were just slightly deformed before sliding of the colloid was reached.[47,48]

In order to further explore the frictional properties of POEGMA brush gradients, friction force-vs-applied load profiles (F_f–L) were recorded at different positions across the substrates. The F_f–L plots measured for POEGMA grafts with $\sigma = 0.09, 0.12, 0.19, 0.22,$ and 0.31 chains nm^{-2} were subsequently compared (Figure 9).

Densely grafted POEGMA brushes ($\sigma = 0.22$ and 0.31) showed low friction and linear F_f–L profiles, following Amontons' law for macroscopic friction: $F_f = \mu L$, where μ represents the coefficient of friction, which was calculated as 0.20 and 0.15, respectively, and L the applied normal load.

The progressive decrease of σ along the POEGMA brush gradient was accompanied by an increase of friction, with F_f–L plots recorded on POEGMA brushes characterized by lower grafting densities, and following sublinear trends (Figure 9).

The influence of grafting density on the frictional behavior of POEGMA grafts could be interpreted by considering the relationship introduced by Busuttil et al.[49] and Nikogeorgos et al.[50] In particular, friction was described as the sum of a load-dependent term, which was associated with "molecular plowing", and derives from the energy dissipation generated
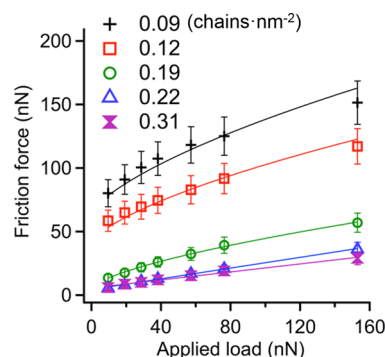
Figure 9. F_f–L data recorded at different positions (corresponding to different σ, as indicated) along the POEGMA brush gradient. The friction force was obtained by averaging the measured lateral force on trace and retrace from friction loops recorded under different applied normal loads (friction = (trace − retrace)/2). Each F_f–L profile resulted from averaging 10 measurements in several positions presenting the same brush grafting density. F_f–L data were recorded in the load range included between 9 and 153 nN. Each F_f–L profile was fitted with the generalized transition equation (GTE) equation (vide infra): for $\sigma = 0.09$ chains nm^{-2} $F_0 = 3.9 \times 10^{-8}$, $\alpha = 1 \pm 0.1$, and $F_a = 1.1 \times 10^{-8}$; for $\sigma = 0.12$ chains nm^{-2} $F_0 = 2.5 \times 10^{-8}$, $\alpha = 1 \pm 0.1$, and $F_a = 8 \times 10^{-9}$; for $\sigma = 0.19$ chains nm^{-2} $F_0 = 1.5 \times 10^{-8}$, $\alpha = 0.5 \pm 0.1$, and $F_a = 5 \times 10^{-9}$; for $\sigma = 0.22$ and 0.31 chains nm^{-2} Amontons' law was applied. During LFM measurements a colloidal probe with normal spring constant of 1 N m^{-1}, torsional spring constant of 1.7×10^{-7} N m, and radius of 8 μm was used.

by a variation of the polymer conformation at the surface, and a shear term, which correlates to the shear strength τ:

$$F_f = \mu(L + F_A) + \tau\pi\left[\frac{R(L + F_A)}{E}\right]^{2/3} \tag{4}$$

where F_A is the adhesion force, R is the radius of the AFM colloidal probe, and E is the apparent modulus of the film. In the case of negligible adhesion, as for densely grafted POEGMA brushes, the second term of eq 4 can be ignored, and the recorded friction follows Amontons' law. A decrease of the values of σ along the gradient was accompanied by a concomitant increase of F_A, making the second term of eq 4 not negligible and thus determining a sublinear regression in the F_f–L profiles. In these circumstances, the F_f–L profiles could be interpreted taking into account the continuum contact mechanics models applied for describing single-asperity contacts in AFM,[43,51] summarized with the generalized transition equation (GTE) introduced by Carpick et al.,[53] which suggests the type of model better describing AFM probe−brush interactions.

$$\frac{a}{a_0} = \left(\frac{\alpha + \sqrt{1 + L/F_A}}{1 + \alpha}\right)^{2/3} \tag{5}$$

where a and a_0 represent the contact radius and the contact radius at zero load, respectively, and α indicates the "transition parameter". Namely, $\alpha = 1$ refers to the Johnson−Kendall−Roberts (JKR) model, which generally applies to materials with high surface energy and undergoing large elastic deformations.[54] $\alpha = 0$ correlates to the Derjaguin−Müller−Toporov (DMT) model, which is usually applied to stiffer and less deformable materials characterized by low surface energy.[55,56] Finally, $0 < \alpha < 1$ indicates a transition regime between the two models. The obtained F_f–L data could be fitted with the GTE

equation by replacing the occurrence of a with $\sqrt{F_f}$ (continuous lines in Figure 9),[53] finally determining the values of α for the low grafting density POEGMA brushes.

Remarkably, on POEGMA brushes characterized by the lowest grafting densities α was 1 ± 0.1 both for $\sigma = 0.09$ and 0.12, indicating JKR contact mechanics. This result was in agreement with the characteristics of loosely grafted POEGMA chains along the gradient, which showed a relatively high content of swelling water (Figure 1) and which could be significantly deformed by the shearing AFM probe (Figure 8). In contrast, POEGMA brushes presenting an "average" grafting density of 0.19 were characterized by $\alpha = 0.5 \pm 0.1$, a value that indicated a transition regime between JKR and DMT models. Hence, the analysis of F_f–L profiles confirmed that the progressive increase in σ across the POEGMA gradient induced a simultaneous reduction of brush deformability and swelling. Denser POEGMA brushes produced a more efficient entropic barrier and thus provided negligible adhesion and low friction compared to their less dense counterparts.

CONCLUSION

Surface-initiated CuCRP has been revealed as a powerful tool to fabricate grafting density gradients of brushes across a single substrate in one pot. This was demonstrated for POEGMA brushes, which are highly relevant surface modifiers for the design of biopassive coatings and cell-sensitive platforms. A gradual variation in the distance between the initiator-bearing substrate and a Cu plate immersed in the polymerization mixture spatially regulated the local concentration of activator species at the propagating chains. This phenomenon, verified by analyzing the concentration of activators near the grafting surface by means of a monolayer of Cu^I-selective ligands, determined the contribution of radical-termination reactions between growing grafts, ultimately generating a grafting-density gradient of POEGMA brushes across the substrate. This distinctive mechanism was also confirmed by monitoring the grafts' thickening rates at specific positions across the sample, the areas closer to the metallic surface showing relatively slow polymer growth compared to regions characterized by larger separations.

The interfacial physicochemical properties of the generated POEGMA brushes could be subsequently investigated along the grafting-density gradient, especially focusing on the swelling, nanomechanical, and nanotribological properties of the grafts. A combination of VASE, AFM nanoindentation, and LFM provided a full characterization of the effects of grafting-density variation on brush swelling, adhesion, stiffness, lateral deformability, and friction. Loosely grafted POEGMA grafts showed high water content and could be significantly deformed by the shearing AFM probe. Friction recorded by LFM was relatively high, and the F_f–L profiles could be interpreted assuming a JKR contact-mechanics model, which is characteristic of compliant materials that display high surface energy. In contrast, the progressive increase of grafting density across the gradient translated into less swollen and more packed POEGMA grafts, which showed higher resistance toward lateral deformation and relatively low friction. In the case of POEGMA brushes presenting the highest grafting density along the fabricated gradient, F_f–L profiles showed a linear progression in accordance with Amontons' law and a coefficient of friction of 0.15.

The proposed fabrication approach and the subsequent characterization highlight how SI-CuCRP is a highly versatile method for synthesizing polymer brushes with precisely defined structural parameters in a relevantly easy and reproducible fashion. When applied to the synthesis of POEGMA grafts, this method yielded gradient brush platforms that allowed a thorough understanding of how brush structural modification translates into variations of physicochemical properties that are highly relevant for the subsequent application of the fabricated coatings. We believe that the accessible, further modulation of catalyst diffusion, e.g. by employing different solvents or by varying the temperature of the polymerization medium, could realistically enable the application of SI-CuCRP for the synthesis of more complex polymer architectures, ranging from polymer brush double gradients to multiblock copolymer films.

■ ASSOCIATED CONTENT

ⓢ Supporting Information

The Supporting Information is available free of charge on the ACS Publications website at DOI: 10.1021/acs.macromol.7b00088.

Chemical characterization of the CSL adsorbate, the AFM-step height measurements, the complete XPS analysis of CSL monolayers, and further lateral force microscopy (LFM) measurements (PDF)

■ AUTHOR INFORMATION

Corresponding Authors

*(R.J.) E-mail rainer.jordan@tu-dresden.de; Ph +49 351 463 37676.

*(E.M.B.) E-mail edmondo.benetti@mat.ethz.ch; Ph +41 44 632 60 50.

ORCID ⓞ

Nicholas D. Spencer: 0000-0002-7873-7905

Edmondo M. Benetti: 0000-0002-5657-5714

Author Contributions

E.S.D. and Y.D. contributed equally.

Notes

The authors declare no competing financial interest.

■ REFERENCES

(1) Bhat, R. R.; Tomlinson, M. R.; Wu, T.; Genzer, J. Surface-Grafted Polymer Gradients: Formation, Characterization, and Applications. In *Surface-Initiated Polymerization II*; Springer-Verlag: Berlin, 2006; pp 51−124.

(2) Genzer, J. Surface-Bound Gradients for Studies of Soft Materials Behavior. *Annu. Rev. Mater. Res.* **2012**, *42* (1), 435−468.

(3) Koo, H. J.; Waynant, K. V.; Zhang, C.; Haasch, R. T.; Braun, P. V. General Method for Forming Micrometer-Scale Lateral Chemical Gradients in Polymer Brushes. *Chem. Mater.* **2014**, *26* (8), 2678−2683.

(4) Tsujii, Y.; Ohno, K.; Yamamoto, S.; Goto, A.; Fukuda, T. Structure and Properties of High-Density Polymer Brushes Prepared by Surface-Initiated Living Radical Polymerization. *Adv. Polym. Sci.* **2006**, *197*, 1−45.

(5) Coad, B. R.; Bilgic, T.; Klok, H.-A. Polymer Brush Gradients Grafted from Plasma-Polymerized Surfaces. *Langmuir* **2014**, *30* (28), 8357−8365.

(6) Kim, M. S.; Khang, G.; Lee, H. B. Gradient Polymer Surfaces for Biomedical Applications. *Prog. Polym. Sci.* **2008**, *33*, 138−164.

(7) Rosenberg, K. J.; Goren, T.; Crockett, R.; Spencer, N. D. Load-Induced Transitions in the Lubricity of Adsorbed Poly(L-Lysine)-*G*-Dextran as a Function of Polysaccharide Chain Density. *ACS Appl. Mater. Interfaces* **2011**, *3* (8), 3020−3025.

(8) Perry, S. S.; Yan, X.; Limpoco, F. T.; Lee, S.; Müller, M.; Spencer, N. D. Tribological Properties of poly(L-Lysine)-Graft-Poly(ethylene Glycol) Films: Influence of Polymer Architecture and Adsorbed Conformation. *ACS Appl. Mater. Interfaces* **2009**, *1* (6), 1224−1230.

(9) Chaudhury, M. K.; Whitesides, G. M. How to Make Water Run Uphill. *Science (Washington, DC, U. S.)* **1992**, *256* (5063), 1539−1541.

(10) Tomlinson, M. R.; Genzer, J. Formation of Grafted Macromolecular Assemblies with a Gradual Variation of Molecular Weight on Solid Substrates. *Macromolecules* **2003**, *36* (10), 3449−3451.

(11) Ma, H.; Hyun, J.; Stiller, P.; Chilkoti, A. Non-Fouling" Oligo(ethylene Glycol)- Functionalized Polymer Brushes Synthesized by Surface-Initiated Atom Transfer Radical Polymerization. *Adv. Mater.* **2004**, *16* (4), 338−341.

(12) Tugulu, S.; Arnold, A.; Sielaff, I.; Johnsson, K.; Klok, H. Protein-Functionalized Polymer Brushes. *Biomacromolecules* **2005**, *6* (3), 1602−1607.

(13) Gunnewiek, M. K.; Di Luca, A.; Bollemaat, H. Z.; van Blitterswijk, C. A.; Vancso, G. J.; Moroni, L.; Benetti, E. M. Creeping Proteins in Microporous Structures: Polymer Brush-Assisted Fabrication of 3D Gradients for Tissue Engineering. *Adv. Healthcare Mater.* **2015**, *4* (8), 1169−1174.

(14) Zhang, T.; Du, Y.; Müller, F.; Amin, I.; Jordan, R. Surface-Initiated Cu(0) Mediated Controlled Radical Polymerization (SI-CuCRP) Using a Copper Plate. *Polym. Chem.* **2015**, *6* (14), 2726−2733.

(15) Yamamoto, S.; Ejaz, M.; Tsujii, Y.; Fukuda, T. Surface Interaction Forces of Well-Defined, High-Density Polymer Brushes Studied by Atomic Force Microscopy. 2. Effect of Graft Density. *Macromolecules* **2000**, *33* (15), 5608−5612.

(16) Yamamoto, S.; Ejaz, M.; Tsujii, Y.; Matsumoto, M.; Fukuda, T. Surface Interaction Forces of Well-Defined, High-Density Polymer Brushes Studied by Atomic Force Microscopy. 1. Effect of Chain Length. *Macromolecules* **2000**, *33* (15), 5602−5607.

(17) Yang, L.; McRae, R.; Henary, M. M.; Patel, R.; Lai, B.; Vogt, S.; Fahrni, C. J. Imaging of the Intracellular Topography of Copper with a Fluorescent Sensor and by Synchrotron X-Ray Fluorescence Microscopy. *Proc. Natl. Acad. Sci. U. S. A.* **2005**, *102*, 11179−11184.

(18) Zhang, T.; She, G.; Qi, X.; Mu, L. A BODIPY-Based Sensor for Hg2+ in Living Cells. *Tetrahedron* **2013**, *69* (34), 7102−7106.

(19) Tompkins, H.; Irene, E. A. *Handbook of Ellipsometry*; Elsevier: 2005.

(20) Butt, H.-J.; Cappella, B.; Kappl, M. Force Measurements with the Atomic Force Microscope: Technique, Interpretation and Applications. *Surf. Sci. Rep.* **2005**, *59* (1−6), 1−152.

(21) Green, C. P.; Lioe, H.; Cleveland, J. P.; Proksch, R.; Mulvaney, P.; Sader, J. E. Normal and Torsional Spring Constants of Atomic Force Microscope Cantilevers. *Rev. Sci. Instrum.* **2004**, *75* (6), 1988.

(22) Hertz, H. Ueber Die Berührung Fester Elastischer Körper. *J. für die reine und Angew. Math. (Crelle's Journal)* **1882**, *1882* (92), 156−171.

(23) Cannara, R. J.; Eglin, M.; Carpick, R. W. Lateral Force Calibration in Atomic Force Microscopy: A New Lateral Force Calibration Method and General Guidelines for Optimization. *Rev. Sci. Instrum.* **2006**, *77* (5), 053701.

(24) Jordan, R.; Ulman, A.; Kang, J. F.; Rafailovich, M. H.; Sokolov, J. Surface-Initiated Anionic Polymerization of Styrene by Means of Self-Assembled Monolayers. *J. Am. Chem. Soc.* **1999**, *121* (5), 1016−1022.

(25) Singh, N.; Cui, X.; Boland, T.; Husson, S. The Role of Independently Variable Grafting Density and Layer Thickness of Polymer Nanolayers on Peptide Adsorption and Cell Adhesion. *Biomaterials* **2007**, *28* (5), 763−771.

(26) Zhang, T.; Du, Y.; Kalbacova, J.; Schubel, R.; Rodriguez, R. D.; Chen, T.; Zahn, D. R. T.; Jordan, R. Wafer-Scale Synthesis of Defined Polymer Brushes under Ambient Conditions. *Polym. Chem.* **2015**, *6* (47), 8176−8183.

(27) Matyjaszewski, K.; Tsarevsky, N. V.; Braunecker, W. A.; Dong, H.; Huang, J.; Jakubowski, W.; Kwak, Y.; Nicolay, R.; Tang, W.; Yoon, J. A. Role of Cu 0 in Controlled/"Living" Radical Polymerization. *Macromolecules* **2007**, *40* (22), 7795−7806.

(28) Konkolewicz, D.; Wang, Y.; Zhong, M.; Krys, P.; Isse, A. A.; Gennaro, A.; Matyjaszewski, K. Reversible-Deactivation Radical Polymerization in the Presence of Metallic Copper. A Critical Assessment of the SARA ATRP and SET-LRP Mechanisms. *Macromolecules* **2013**, *46* (22), 8749−8772.

(29) Peng, C.-H.; Zhong, M.; Wang, Y.; Kwak, Y.; Zhang, Y.; Zhu, W.; Tonge, M.; Buback, J.; Park, S.; Krys, P.; Konkolewicz, D.; Gennaro, A.; Matyjaszewski, K. Reversible-Deactivation Radical Polymerization in the Presence of Metallic Copper. Activation of Alkyl Halides by Cu 0. *Macromolecules* **2013**, *46* (10), 3803−3815.

(30) Ding, S.; Floyd, J. A.; Walters, K. B. Comparison of Surface Confined ATRP and SET-LRP Syntheses for a Series of Amino (Meth)acrylate Polymer Brushes on Silicon Substrates. *J. Polym. Sci., Part A: Polym. Chem.* **2009**, *47* (23), 6552−6560.

(31) Xie, Y.; He, C.; Liu, L.; Mao, L.; Wang, K.; Huang, Q.; Liu, M.; Wan, Q.; Deng, F.; Huang, H.; Zhang, X.; Wei, Y. Carbon Nanotube Based Polymer Nanocomposites: Biomimic Preparation and Organic Dye Adsorption Applications. *RSC Adv.* **2015**, *5* (100), 82503−82512.

(32) Wu, T.; Efimenko, K.; Vlček, P.; Šubr, V.; Genzer, J. Formation and Properties of Anchored Polymers with a Gradual Variation of Grafting Densities on Flat Substrates. *Macromolecules* **2003**, *36* (7), 2448−2453.

(33) Li, B.; Yu, B.; Huck, W. T. S.; Liu, W.; Zhou, F. Electrochemically Mediated Atom Transfer Radical Polymerization on Nonconducting Substrates: Controlled Brush Growth through Catalyst Diffusion. *J. Am. Chem. Soc.* **2013**, *135* (5), 1708−1710.

(34) Konkolewicz, D.; Wang, Y.; Krys, P.; Zhong, M.; Isse, A. A.; Gennaro, A.; Matyjaszewski, K. SARA ATRP or SET-LRP. End of Controversy? *Polym. Chem.* **2014**, *5* (15), 4409.

(35) Matyjaszewski, K.; Nanda, A. K.; Tang, W. Effect of [Cu II] on the Rate of Activation in ATRP. *Macromolecules* **2005**, *38* (5), 2015−2018.

(36) Pyun, J.; Kowalewski, T.; Matyjaszewski, K. Synthesis of Polymer Brushes Using Atom Transfer Radical Polymerization. *Macromol. Rapid Commun.* **2003**, *24* (18), 1043−1059.

(37) Hucknall, A.; Simnick, A. J.; Hill, R. T.; Chilkoti, A.; Garcia, A.; Johannes, M. S.; Clark, R. L.; Zauscher, S.; Ratner, B. D. Versatile Synthesis and Micropatterning of Nonfouling Polymer Brushes on the Wafer Scale. *Biointerphases* **2009**, *4* (2), FA50.

(38) Hucknall, A.; Rangarajan, S.; Chilkoti, A. In Pursuit of Zero: Polymer Brushes That Resist the Adsorption of Proteins. *Adv. Mater.* **2009**, *21* (23), 2441−2446.

(39) Tugulu, S.; Klok, H.-A. Stability and Nonfouling Properties of Poly(poly(ethylene Glycol) Methacrylate) Brushes under Cell Culture Conditions. *Biomacromolecules* **2008**, *9* (3), 906−912.

(40) Halperin, A. Polymer Brushes That Resist Adsorption of Model Proteins: Design Parameters. *Langmuir* **1999**, *15* (7), 2525−2533.

(41) Goodman, D.; Kizhakkedathu, J. N.; Brooks, D. E. Attractive Bridging Interactions in Dense Polymer Brushes in Good Solvent

Measured by Atomic Force Microscopy. *Langmuir* **2004**, *20* (6), 2333−2340.

(42) Landherr, L. J. T.; Cohen, C.; Agarwal, P.; Archer, L. A. Interfacial Friction and Adhesion of Polymer Brushes. *Langmuir* **2011**, *27* (15), 9387−9395.

(43) Sui, X.; Chen, Q.; Hempenius, M. A.; Vancso, G. J. Probing the Collapse Dynamics of Poly(N-Isopropylacrylamide) Brushes by AFM: Effects of Co-Nonsolvency and Grafting Densities. *Small* **2011**, *7* (10), 1440−1447.

(44) Gunnewiek, M. K.; Ramakrishna, S. N.; di Luca, A.; Vancso, G. J.; Moroni, L.; Benetti, E. M. Stem-Cell Clinging by a Thread: AFM Measure of Polymer-Brush Lateral Deformation. *Adv. Mater. Interfaces* **2016**, *3* (3), 1500456.

(45) Ramakrishna, S. N.; Cirelli, M.; Kooij, E. S.; Klein Gunnewiek, M.; Benetti, E. M. Amplified Responsiveness of Multilayered Polymer Grafts: Synergy between Brushes and Hydrogels. *Macromolecules* **2015**, *48* (19), 7106−7116.

(46) Li, A.; Ramakrishna, S. N.; Nalam, P. C.; Benetti, E. M.; Spencer, N. D. Stratified Polymer Grafts: Synthesis and Characterization of Layered "Brush" and "Gel" Structures. *Adv. Mater. Interfaces* **2014**, *1* (1), 1300007.

(47) Rabin, Y.; Alexander, S. Stretching of Grafted Polymer Layers. *EPL (Europhysics Lett.* **1990**, *13* (1), 49.

(48) Doyle, P. S.; Shaqfeh, E. S. G.; Gast, A. P. Rheology of Polymer Brushes: A Brownian Dynamics Study. *Macromolecules* **1998**, *31* (16), 5474−5486.

(49) Busuttil, K.; Geoghegan, M.; Hunter, C. A.; Leggett, G. J. Contact Mechanics of Nanometer-Scale Molecular Contacts: Correlation between Adhesion, Friction, and Hydrogen Bond Thermodynamics. *J. Am. Chem. Soc.* **2011**, *133* (22), 8625−8632.

(50) Nikogeorgos, N.; Hunter, C. A.; Leggett, G. J. Relationship Between Molecular Contact Thermodynamics and Surface Contact Mechanics. *Langmuir* **2012**, *28* (51), 17709−17717.

(51) Raftari, M.; Zhang, Z.; Carter, S. R.; Leggett, G. J.; Geoghegan, M. Frictional Properties of a Polycationic Brush. *Soft Matter* **2014**, *10* (16), 2759.

(52) Marti, A.; Haehner, G.; Spencer, N. D. Sensitivity of Frictional Forces to pH on a Nanometer Scale: A Lateral Force Microscopy Study. *Langmuir* **1995**, *11* (12), 4632−4635.

(53) Carpick, R. W.; Ogletree, D. F.; Salmeron, M. A General Equation for Fitting Contact Area and Friction vs Load Measurements. *J. Colloid Interface Sci.* **1999**, *211* (2), 395−400.

(54) Johnson, K. L.; Kendall, K.; Roberts, A. D. Surface Energy and the Contact of Elastic Solids. *Proc. R. Soc. London, Ser. A* **1971**, *324* (1558), 301−313.

(55) Derjaguin, B. V.; Muller, V. M.; Toporov, Y. P. Effect of Contact Deformations on the Adhesion of Particles. *J. Colloid Interface Sci.* **1975**, *53* (2), 314−326.

(56) Chyasnavichyus, M.; Young, S. L.; Tsukruk, V. V. Probing of Polymer Surfaces in the Viscoelastic Regime. *Langmuir* **2014**, *30* (35), 10566−10582.